Journal of Hydrology 598 (2021) 126473

Contents lists available at ScienceDirect

Journal of Hydrology

journal homepage: www.elsevier.com/locate/jhydrol

Research papers

Trends of evaporation in Brazilian tropical reservoirs using remote sensing

Italo Sampaio Rodrigues [a,*], Carlos Alexandre Gomes Costa [b], Iran Eduardo Lima Neto [c], Christopher Hopkinson [d]

[a] Space and Physical Science, University of Lethbridge, Canada
[b] Department of Agricola Engineering, Federal University of Ceará (UFC), Brazil
[c] Department of Hydraulic and Environmental Engineering, Federal University of Ceará (UFC), Brazil
[d] Department of Geography, University of Lethbridge, Canada

ARTICLE INFO

This manuscript was handled by Emmanouil Anagnostou, Editor-in-Chief, with the assistance of Viviana Maggioni, Associate Editor

Keywords:
Climate change
Evaporation
Hydroclimatic data
Reservoirs
Trends

ABSTRACT

This paper aims to analyze the trends (Mann-Kendall test) of evaporation and climatological variables, including air temperature, relative humidity and wind speed in four reservoirs located in the Brazilian Northeast. The evaporation was estimated through remote sensing using the Surface Energy Balance System for Water (Aqua-SEBS) model from 1985 to 2018. In addition, it was verified which meteorological parameter has the highest correlation (R^2) with the evaporation in order to assess why this process is changing throughout the years in each reservoir. The model performed well, with root mean square error (RMSE) $\leq$ 1.25 mm/day, percent bias (PBIAS) $\leq$ 13.70% and coefficient of determination (R^2) $\geq$ 0.51. One reservoir located closer to a coastal zone presented a positive trend (+0.24 mm/34 years), corroborating the measurements of a reference class A pan, and Penman-Monteith equation, while the others, located closer to industrial areas, displayed negative trends (−0.26 to −0.080 mm/34 years). This reduced evaporation was attributed to the impact of industrial pollutant release to the atmosphere, while the increasing effect in the other reservoir was due to its proximity to the coast, which implies an air renewal as the sea breeze contributes for an improvement in the air quality. The meteorological data also presented positive and negative correlations: Temperature exhibited a positive trend (+0.57 °C/34 years), whereas humidity (−4.83%) and wind speed (−0.29 m/s), a negative trend. Evaporation displayed moderate coefficient of determination ($R^2 > 0.31$) with wind speed and humidity. Yet, the reduction of evaporation may be associated with a possible counterbalancing effect of wind speed over humidity. Overall, the results contribute to a better understanding of evaporation trends in a water-scarce region and can be used in a water resources management context as the increasing/reduction of evaporation might significantly impact water availability in this area.

1. Introduction

Evaporation is an important component of the hydrological cycle and influences the availability of water for agriculture, domestic and industrial consumption (Konapala et al., 2020). Since there are>304 billion reservoirs in the world (Downing et al., 2006), evaporation from these water bodies plays a vital role in global energy distribution and the hydrological cycle (Rong et al., 2013).

The Brazilian Northeast Region (BNR) suffers constant water resource vulnerability. With approximately 60 million inhabitants, this region is recognized as the most populated semi-arid region in the world (Lima Neto, 2019). In the state of Ceará, one of the nine Brazilian federal states within BNR, over 25,000 small, medium and large reservoirs have been built to provide reliable water access during the dry season (Lima Neto et al., 2011; Mamede et al., 2018). However, the quantification of evaporation in these reservoirs is usually limited to estimates from Class A pan measurements (Campos et al., 2016a). Furthermore, there is no study reporting the trends of reservoir evaporation in BNR.

There are several classical approaches to quantifying lake evaporation: the aerodynamic, energy balance, combined aerodynamic and energy balance models and Eddy Covariance (McMahon et al., 2016; Metzger et al., 2018). Alternatively, Mesquita et al. (2020) recently applied hydrodynamic modelling to assess lake evaporation. Using Remote Sensing (RS), evaporation assessments can be made over large areas and provide a tool for large-scale water resources planning and management (Losgedaragh and Rahimzadegan, 2018). In addition, the

* Corresponding author at: Space and Physical Science, Department of Geography, University of Lethbridge, Canada.
E-mail address: italo.rodrigues@uleth.ca (I.S. Rodrigues).

https://doi.org/10.1016/j.jhydrol.2021.126473
Received 30 November 2020; Received in revised form 7 April 2021; Accepted 16 May 2021
Available online 19 May 2021

use of RS may improve the understanding of spatiotemporal dynamics of lake evaporation, since the sequence of scenes can exceed 40 years (Senay et al., 2017).

Climate change has the potential to impact evaporation and water availability (Konapala et al., 2020). Previous studies have reported contrasting trends of increasing (Pourmansouri and Rahimzadegan, 2020; Nouri et al., 2017) and decreasing (Xu et al., 2018; Liu et al., 2004) evaporation across various regions of the globe, which has been referred to as the "evaporation paradox" (Brutsaert and Parlange, 1998). Moreover, lake evaporation rates depend on several climatological variables such as air temperature, relative humidity and wind speed (Friedrich et al., 2018). Thus, the identification of long term evaporation trends could help quantify the potential impacts of climate change on reservoir evaporation and water availability in water-scarce regions such as BNR.

The objectives of this paper are to assess the trends of evaporation in four Brazilian tropical reservoirs using RS, and correlate these with trends in the climatological variables of air temperature, relative humidity and wind speed. This work is valuable, since an understating of lake evaporation trends is needed for BNR water resources management. To the authors' knowledge, there have been no similar assessments in the BNR.

2. Methodology

2.1. Study area

Four reservoirs were studied: Santo Anastácio (volume 0.3 hm^3 and greatest depth 3.8 m) (Fraga et al., 2020), Gavião (33.3 hm^3 and 16 m), Riachão (47 hm^3 and 46 m) and Pacoti (380 hm^3 and 28 m). These reservoirs are located in the state of Ceará, Brazil, and are considered tropical-coastal reservoirs. This region presents a historical average of: temperature 26 °C, solar duration 2800 h/year, rainfall regime 1600 mm/year, wind speed 4 m/s, humidity 78% (INMET, 2019). Santo Anastácio does not supply any community because it is extremely polluted by urban runoff (Araújo and Lima Neto, 2018; Fraga et al., 2020). Otherwise, Gavião, Riachão and Pacoti are strategic reservoirs that are the final stage of the main water supply complex in the State of Ceará. These three reservoir hydrographs are artificially perennialized by the "Eixão das Águas", a water transboundary system from the Castanhão reservoir, the largest reservoir in the state (COGERH, 2020). Together, these reservoirs supply the metropolitan region of Fortaleza with a population of more than four million people (IPECE, 2018).

2.2. Modeling framework

The trend analysis of evaporation using Remote Sensing requires five steps, as shown in Fig. 2: i) Acquisition of meteorological data (air temperature, wind speed and humidity), observed evaporation data (Class A pan) and Penman-Monteith estimates for validation purposes; ii) acquisition of scenes from Landsat 5 and 8 satellites; iii) application of the model (AquaSEBS); iv) statistical analysis of modeled and measured data and; v) analysis of temporal variations in evaporation.

The unsupervised k-means classification algorithm was used to vectorize the surface area of the case study reservoirs. The k-means approach was chosen because it is known to reliably discriminate water bodies (Campos et al., 2016b). The Raster Calculator tool was used to apply the models, generating the spatialized evaporation estimates for the reservoirs. All geoprocessing operations were carried out in QGIS 3.14.

2.3. Data sources

The evaporation analysis was carried out for the period 1985 to 2018. Only scenes containing at least three visible reservoirs were used. In total, 29 scenes were used, twenty from Landsat 5 and nine from Landsat 8 (Fig. 2). All scenes were acquired through the United States Geological Survey (USGS). The meteorological data and Class A pan evaporation were acquired through the Federal University of Ceará which has measurements since 1966.

2.4. AquaSEBS

AquaSEBS (Abdelrady et al., 2016) was adapted from the SEBS (Surface Energy Balance System) (Su, 2002) model to estimate evaporation in fresh water. SEBS was created to estimate evapotranspiration (in vegetation and soil) and the main difference between these two models is the way heat flux is handled; wet (latent) for water and dry (sensible) for vegetation and soil. AquaSEBS was chosen as it has been validated in several water bodies at different environmental conditions (Abdelrady et al., 2016; Losgedaragh and Rahimzadegan, 2018) (Eq. (1)).

$$\lambda E_{wet} = R_n - G_0 - H_{wet} \quad (1)$$

λE_{wet} represents the latent heat flux over the water surface (W/m^2), R_n is the net radiation incident upon the water surface (W/m^2), G_0 is the internal water body heat flux (W/m^2) and H_{wet} is the sensible heat flux at the water surface (W/m^2). Both AquaSEBS and SEBS require three types of data: i) Remote Sensing – surface emissivity, surface albedo and surface temperature of the water, ii) Meteorological - air temperature, relative humidity and wind speed, iii) Radiation - incoming short wave and longwave radiation. For the temporal assessment, scenes from the Landsat 5 (Thematic Mapper - TM) and Landsat 8 (Optical Land Imager - OLI) satellite sensors were used. These sensors have distinct technical characteristics (radiometric, spectral and spatial resolution of the thermal band), making it necessary to use methodological adjustments to acquire some parameters in the application of the model. To estimate the net radiation (R_n), Eq. (2) was used for both the TM and OLI sensors

$$R_n = (1-\alpha)R_{s\downarrow} + \varepsilon R_{L\downarrow} - \varepsilon_a \sigma T_s^4 \quad (2)$$

α is the albedo, $R_{s\downarrow}$ is the incoming shortwave solar radiation (W/m^2), $R_{L\downarrow}$ incoming longwave radiation (W/m^2), ε is the emissivity (and absorptivity) of the surface, ε_a represents atmospheric emissivity (and absorptivity), σ is the Stefan-Boltzmann constant ($5.67*10^{-8}$) (W/m^2K^4) and Ts is the surface temperature (°C) of the water body (one of the most sensitive parameters). To estimate the parameters of R_n for the TM sensor, we used: α(Chandler and Markham, 2003; Duffie and Beckman 1980; Allen et al., 2002; Tasumi, 2003; Bastiaanssen, 2000), $R_{s\downarrow}$(Allen et al., 2002), $R_{L\downarrow}$ (Bastiaanssen et al., 1998), ε (Allen et al., 2002) and ε_a (Bastiaanssen et al., 1998). For the OLI sensor, slight modifications were used to calculate α(Missions, 2016; Silva et al., 2016; Allen et al., 2002; Tasumi, 2003; Bastiaanssen, 2000). The algorithms from Malaret et al. (1985) and Avdan and Jovanovska (2016) were used to calculate Ts for TM and OLI, respectively. These algorithms were selected to estimate surface temperature due to their demonstrated accuracy when compared to measured surface temperature data. OLI displayed R^2 = 0.65 (Avdan and Jovanovska, 2016) and TM R^2 = 0.82 (Malaret et al. 1985). G_0 was calculated following Abdelrady et al. (2016). H_{wet} was estimated according to Su (2002) (Eq. (3)).

$$H_{wet} = \frac{\left[(R_n - G_0) - \frac{\rho_a * C_p * (e_s - e_a)}{r_{ew} * \gamma}\right]}{\left(1 + \frac{\Delta}{\gamma}\right)} \quad (3)$$

C_p is the specific heat capacity constant of the air (1004 J/Kg.°C), ρ_a is the air density 1.184 Kg/m^3 (Shelquist, 2009), γ is the psychrometric constant, (hPa/°C) (reference value for this parameter γ = 0.65 hpa/°C), Δ is the rate of change of the saturation vapor pressure with the temperature (hPa/°C), r_{ew} is the external resistance, a value that depends on the Monin-Obukhov length, this represents the parameterization using the variables of wind friction and sensible heat flux. The detailed process to estimate H_{wet} is described in Abdelrady et al. (2016) and Su (2002).

Using Eq. (1), the latent heat flux over the reservoirs was calculated.

Then Eq. (4) was applied to calculate the evaporative fraction (EF), which is the ratio of latent heat flux to the available energy (Abdelrady et al., 2016). Subsequently, the amount of latent heat absorbed by the water body was determined (λE_{daily}), Eqs. (5) and (6) was used to estimate daily spatial evaporation. ρ_w represents the water density, considered 1,000 kg/m^3 and λ is the latent heat of vaporization (MJ/kg).

$$EF = \frac{\lambda E}{(R_n - G_0)} \tag{4}$$

$$\lambda E_{daily} = 86400{*}10^3{*}EF{*}(R_n - G_0) \tag{5}$$

$$E = \frac{\lambda E_{daily}}{\lambda{*}\rho_w} \tag{6}$$

2.5. Input climatological and reference evaporation datasets

The meteorological data (vapor pressure, relative humidity and wind speed) for the reservoirs and the first reference evaporation, Class A pan, were obtained in Fortaleza Weather Station. Both are located at the Federal University of Ceará (UFC), being about 1 km from Santo Anastácio, 15 km from Gavião reservoir, 25 km from Riachão, 30 km from Pacoti. An adjustment coefficient $K_p = 0.7$ for the Class A pan was assumed (Linacre, 1994; Finch and Calver, 2008), as usually considered for tropical regions (Campos et al., 2016a), in order to account for the effects of heat exchange between the edges of the pan and the water.

The Penman-Monteith (Penman, 1948) equation was used as a reference (Eq. (7)).

$$E = \beta \frac{\Delta}{\Delta + \gamma} \frac{R_n - G_0}{\lambda} \tag{7}$$

β is the Priestly-Taylor empirically derived constant (1.26), and the remaining parameters are equivalent to those described for the AquaSEBS model. This equation was chosen to provide a reference estimate because it estimates evaporation with high accuracy in regions with a similar climate to the study area (McJannet et al., 2013).

2.6. Statistical performance

Three parameters were used to analyze the models' performance: Root mean square error (RMSE), percent bias (PBIAS), and coefficient of determination (R^2). The RMSE indicates the similarity between measured and estimated data using models, in which the ideal value is equal to zero. The PBIAS measures the average tendency of the modeled data to be greater or smaller than the corresponding measured data (Gupta et al., 1999). The closer the PBIAS value is to zero, the more accurate the model. According to Moriasi et al. (2007), values of PBIAS can be considered satisfactory within a limit of variation of ± 25%. R^2 varies from 0 to 1, the closer to 1, the greater the correlation between observed and modeled data. In order to apply these tests, the average of the evaporation pixels resulting from the model was used to represent the simulated data.

2.7. Trends in evaporation and proportion of variance with climatological parameters

This analysis aims to assess linear regression (R^2) between the average modeled evaporation (AquaSEBS) with the climatic parameters (air temperature, wind speed and relative humidity). From this analysis, it was verified which climatological factor has the highest correlation/impact with/on the evaporation from each reservoir.

Knowing the climatological parameter with the best correlation with evaporation for each reservoir, a temporal analysis of this parameter was carried out to investigate the trends over 34 years. The trend analysis was performed using the Mann-Kendall method (Kendall, 1975; Mann, 1945), which is a nonparametric test to identify a trend in a series (Eqs. (8)–(11)).

$$S = \sum_{k=1}^{n-1} \sum_{j=k+1}^{n} sign(x_j - x_k) \tag{8}$$

$$sign(x_j - x_k) = \begin{cases} 1(x_j - x_k) > 0 \\ 0(x_j - x_k) = 0 \\ -1(x_j - x_k) < 0 \end{cases} \tag{9}$$

$$Var(S) = \{ [n(n-1)(2n+5)] - \sum_{i=1}^{m} t_i(t_i - 1)(2t_i + 5) \} / 18 \tag{10}$$

$$Z = \begin{cases} S - 1/\sqrt{Var(S)}\, S > 0 \\ 0 S = 0 \\ S + 1/\sqrt{Var(S)}\, S < 0 \end{cases} \tag{11}$$

S represents the Mann-Kendall statistics, n denotes data set length, x_j and x_k are the sequential data values, t_i is the number of ties of extent i, m is number of the tied groups and Z is the standardized Mann-Kendall statistics. The null hypothesis for this test is that there is no trend in the series, such that the three hypotheses evaluated are: i) no trend, ii) positive trend, iii) negative trend. A significance level of $p = 0.05$ was adopted. The Mann-Kendall test was also employed with climatological variables (air temperature, wind speed and relative humidity) and with modeled and measured evaporation. This allowed an evaluation of whether reservoir evaporation increased, decreased or remained stable throughout the study period (1985–2018), as well as an analysis of the causes of any change. Any patterns that resulted from the trend analysis, were then extrapolated forwards for 100 and 500 years, simulating the impact of these trends into the future.

Table 1
Performance of modeled evaporation (AquaSEBS) compared to reference data (Class A pan and Penman-Monteith) for each reservoir.

	Class A pan (Kp = 0.7)			Penman-Monteith		
	R^2	PBIAS (%)	RMSE (mm/day)	R^2	PBIAS (%)	RMSE (mm/day)
Santo Anastacio	0.55	3.7	0.93	0.51	13.7	1.25
Gavião	0.55	5.9	0.89	0.58	11.9	1.15
Riachão	0.56	4	0.87	0.61	10.7	1.08
Pacoti	0.62	4.1	0.81	0.65	9.5	1.00

3. Results and discussion

3.1. Statistical analysis

The AquaSEBS model produced errors (RMSE) between 0.81 and 1.25 mm/day in the four study reservoirs relative to the Class A pan (K_p = 0.7) and Penman-Monteith equation (Table 1). PBIAS from both reference estimates suggested that AquaSEBS tended to underestimate evaporation in all reservoirs, with variations ranging from 3.7% to 5.9% for Class A pan and 9.5% to 13.7% for Penman-Monteith. All modeled evaporation showed R^2 greater than or equal to 0.51. From these statistical performances, it can be inferred that the AquaSEBS model produces reasonable estimates of reservoir evaporation. However, the apparent underestimation could be due to a known tendency for the Penman-Monteith model to overestimate (+2%) evaporation in tropical regions (McJannet et al., 2013). Fig. 3presents a box diagram of the modeled evaporation and reference data.

The precision of the AquaSEBS model obtained in the present study was similar to that in previous studies. For instance, Abdelrady et al. (2016) applied AquaSEBS in the Victoria reservoir (Tropical Climate), Africa, satisfactorily estimating the measured data with an RMSE of 1.50 mm/day. Losgedaragh and Rahimzadegan (2018) used AquaSEBS to estimate evaporation in the AmirKabir reservoir (Semi-arid climate), Iran, obtaining small errors of RMSE 0.62 mm/day and R^2 0.93.

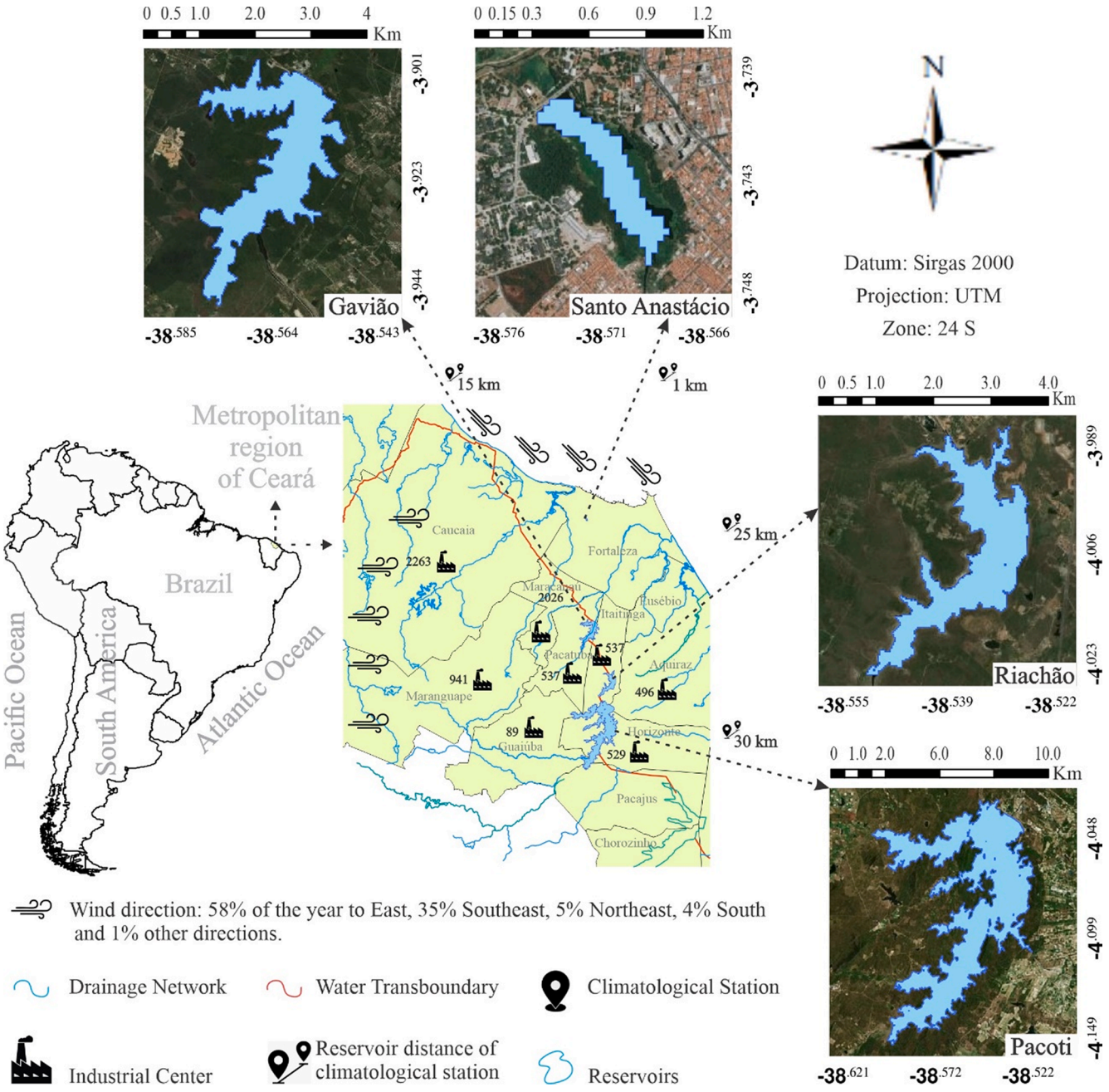

Fig. 1. Location map of the reservoirs under study.

The small underestimation of the AquaSEBS model in the reservoirs here might be related to their water quality, as suggested by Mesquita et al. (2020), who found Class A pan coefficients K_p decreasing from about 0.7 to 0.6 as phosphorus concentration increased in the Santo Anastácio reservoir. Note that all the studied reservoirs are artificially perennialized and receive high phosphorus loads, which resulted in eutrophic and hypereutrophic conditions, as reported by Araújo et al. (2019), Coelho et al. (2017), and COGERH (2020).

Abdelrady et al. (2016) also found that a high concentration of salts (240 g/L) reduced evaporation by up to 27% in the Great Salt Lake (USA) and 1% in the open sea (34.7 g/L). Al-Shammiri (2002) found that the rates of evaporation in freshwater reached double the rates of evaporation of seawater.

Another influence of water pollution and eutrophication is the reduction of albedo and light penetration into the water body due to high turbidity, along with floating macrophytes that can prevent the passage of light, which alters the available radiant energy inputs from the sun (Havens and Ji, 2018; Jin et al., 2004; Mesquita et al., 2020). In other evaporation studies it is noted that evaporation rate rises as turbidity reduces (Morton, 1986; Finch and Hall, 2001).

The results and observations from other studies (noted above) suggest that the AquaSEBS model has produced a reasonable estimate of local evaporation, given the reference evaporation estimation methods (Penman-Monteith and Class A pan) do not consider the potential influences of pollution, which may be a factor across the four studied reservoirs.

3.2. *Influence of climatological variables on evaporation and its temporal change*

All study reservoirs have at least 30 years of data, which is a required period for climate normal and change analysis in a region (Maclean

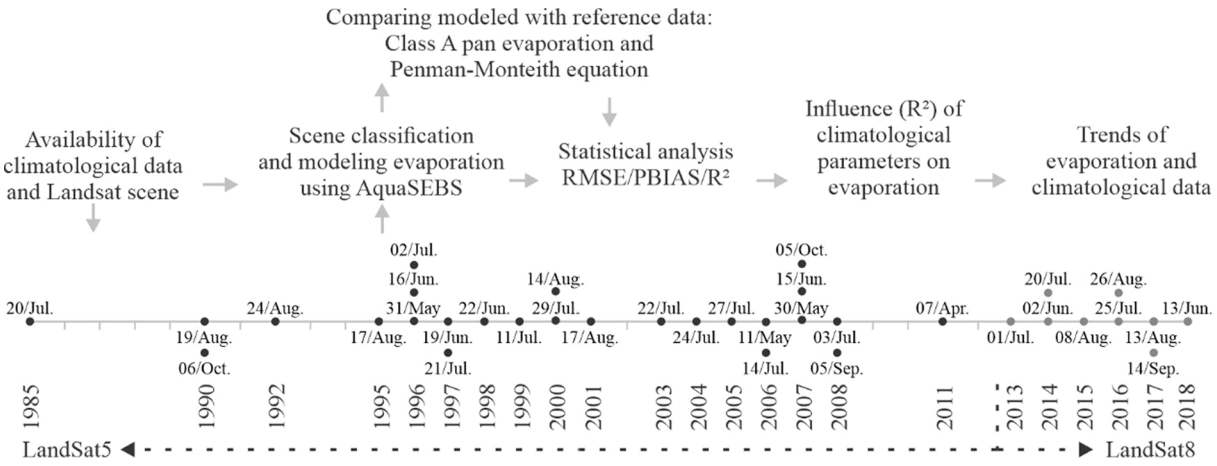

Fig. 2. Methodological flowchart used for evaporation analysis using remote sensing (RS).

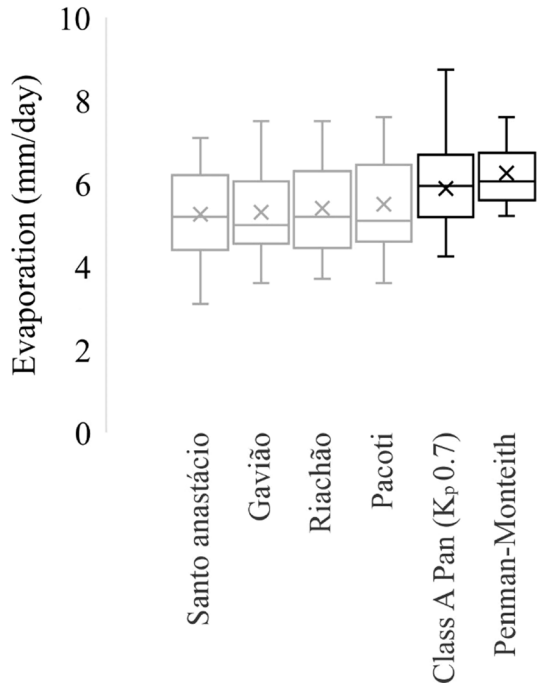

Fig. 3. Box diagrams of average modeled evaporation for the period of 1985–2018 (AquaSEBS) for the four studied reservoirs and the two-reference data.

et al., 2017). Air temperature demonstrated the lowest correlations with evaporation, with R^2 ranging from 0.09 to 0.14 (Fig. 4). Meanwhile, wind speed presented moderate linear regression with evaporation for Santo Anastácio ($R^2 = 0.40$), Gavião ($R^2 = 0.37$), Riachão ($R^2 = 0.42$) and Pacoti ($R^2 = 0.38$). These mid-range regression results can be explained because the Northeast Brazilian coast records the highest wind speeds in Brazil, with an annual average of 4.0 m/s. The humidity also presented similar moderate correlations in all reservoirs: Santo Anastácio ($R^2 = 0.40$), Gavião ($R^2 = 0.33$), Riachão ($R^2 = 0.40$) and Pacoti ($R^2 = 0.31$). Annual average humidity in the region is considered high (67%), which is directly influenced by the proximity of the Atlantic Ocean (Andrade et al., 2020).

The negative correlation between humidity and evaporation (Fig. 4) is expected since high humidity means elevated water vapour pressure in the atmosphere, which inhibits evaporation. The R^2 results between the climatological parameters and the modeled evaporation for the four reservoirs were similar, due to their proximity and comparable weather conditions.

Fig. 5 indicates that the evaporation of the Santo Anastácio reservoir has tended to increase slightly over time. Evaporation model results (AquaSEBS, +0.24 mm in 34 years) followed the same trend as observed data (Class A pan Kp 0.7; +0.43 mm in 34 years) and modelled by Penman-Monteith (+0.30 mm in 34 years). This is consistent with an increase in global air temperatures during the same period (Hansen et al., 2010), which is consistent with the greenhouse effect (Ohmura and Wild, 2002). Note that from 1961 to 1990 there was a 0.50 °C increase in the temperature of the Northeast Brazil, where the studied reservoirs are located. However, Figs. 6–8 indicate a reduction of evaporation along the years in the reservoirs Gavião (−0.14 mm in 34 years), Riachão (−0.26 mm in 34 years), and Pacoti (−0.08 mm in 34 years). While some authors suggest that evaporation has been reducing over this period (Peterson et al., 1995; Chattopadhyay and Hulme, 1997; Lawrimore and Peterson, 2000; Liu et al., 2004), we need to address the inconsistent trend in reservoir evaporative loss between the Santo Anastácio (and the Class A pan) and the other three reservoirs?

The reduction in evaporation observed in the Gavião, Riachão and Pacoti reservoirs might be related to the "global dimming" effect, a consequence of the high incidence of gases/aerosols in the atmosphere, causing an increase in the amount of the local cloudiness, and reducing the heating influence of solar radiation on local water body evaporation (Stanhill and Cohen, 2001). The above-mentioned reservoirs are located close to the industrial centers of Maracanaú (2026 industries), Pacatuba (537 industries), Horizonte (529 industries), Aquiraz (496 industries), Itaitinga (275 industries) and Guaiúba (89 industries), where high gas release to the atmosphere is observed (IPECE, 2017) (see Fig. 1). As reported by Freitas et al. (2016), air quality in these industrial areas is worse than observed in the city of Fortaleza, where the Santo Anastácio reservoir is located. Moreover, the Santo Anastácio reservoir is closer to the coast, which implies that air renewal due to sea breeze contributes for an additional improvement in the air quality. Therefore, air pollution and regional dimming is a plausible explanation for reduced evaporative loss in the Gavião, Riachão and Pacoti reservoirs. Meanwhile, higher air quality around the Santo Anastácio reservoir has allowed more solar radiation to the water body surface, thus enabling air temperature increases to drive an upward trend evaporation, which aligns with the observations from the reference Class A pan.

Liu et al. (2004) found that the evaporation of 85 Class A pans in China, between 1955 and 2000, had decreased at an average rate of 29.3 mm per decade. Roderick and Farquhar (2004) observed, in regions with large industrial centers in Australia, that evaporation reduced by an average of 4.3 mm between 1970 and 2002. This reduction in evaporation was also observed in Canada (Burn and Hesch, 2007), India (Chattopadhyay and Hulme, 1997), Italy (Moonen et al., 2002), Turkey

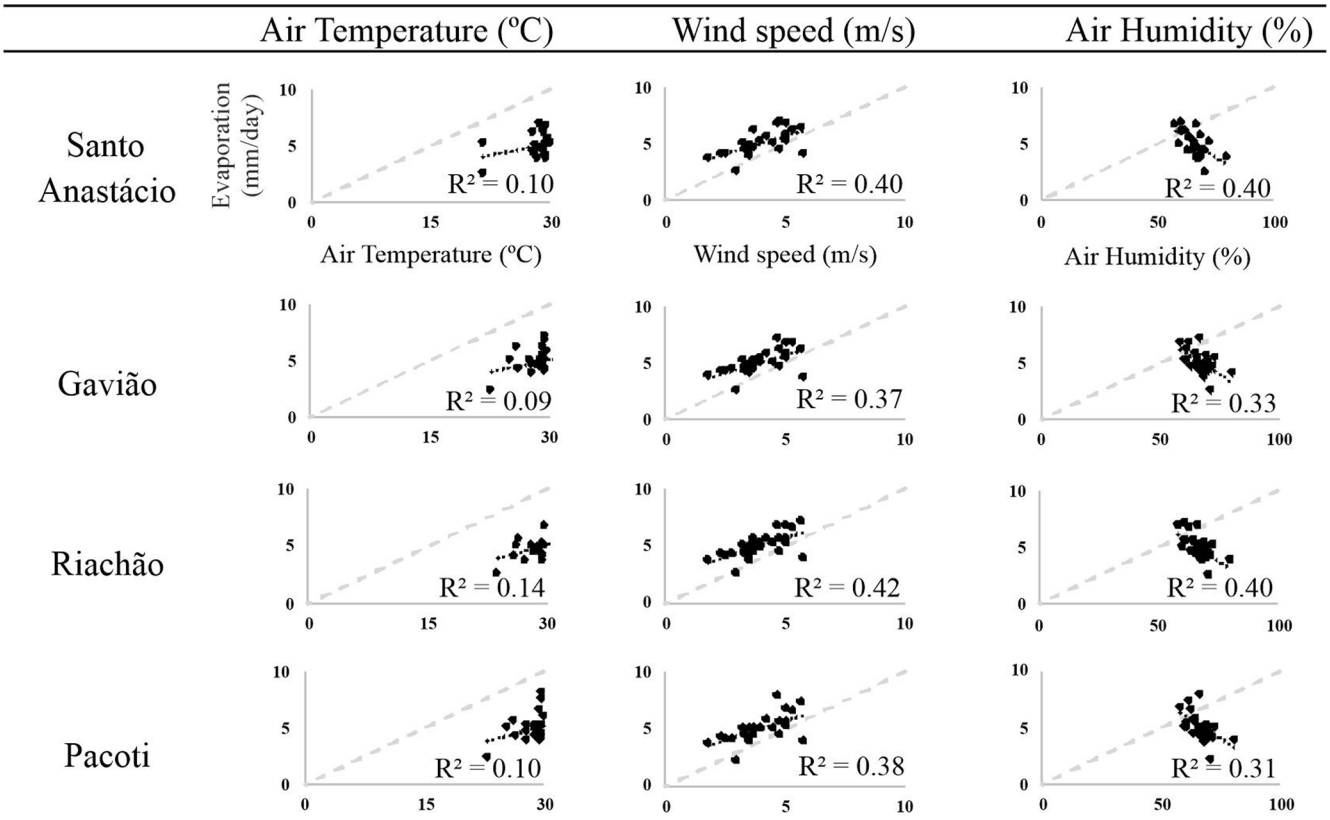

Fig. 4. Correlation (R^2) between modeled evaporation (AquaSEBS) and air temperature, wind speed and humidity.

(Ozdogan and Salvucci, 2004), Puerto Rico (Harmsen et al., 2004), New Zealand (Roderick and Farquhar, 2005), Thailand (Tebakari et al., 2005) and in other highly industrialized countries and regions with high rates of gas emissions (Fu et al., 2009; Miralles et al., 2014).

However, this reduction did not occur homogeneously throughout the world, since many countries are not highly industrialized and do not produce large quantities of gases. Underdeveloped or emerging countries can display the opposite effect, as they do not generate enough gases in the atmosphere to reduce the incidence of solar radiation, potentially resulting in higher evaporation rates. Roderick and Farquhar (2004) (from 1970 to 2002) observed that in the regions of Australia without industrial centers, there was a positive trend in evaporation of 26 to 30 mm. In Israel, Cohen et al. (2002) found a positive trend in local evaporation. Xu et al. (2005) also found an increase in evaporation in the Center and Southwest of China, less industrialized regions of the country, during the period from 1971 to 2000.

Zhao and Gao (2019) found between 1984 and 2015, in 721 US reservoirs, that there was a small increase in evaporation, 0.0076 mm/year (0.24 mm in 31 years). This positive trend in the USA, an industrialized country, can be explained by the significant spatial heterogeneity of the reservoirs, being largely located in regions where there is no or minimal nearby industrialization. Guo et al. (2019) observed an increase in evaporation between 1961 and 2015 of Lake Siling Co, Tibet, with an annual trend of 0.50 mm/year. A positive evaporation trend was also observed in Benin, West Africa (Hounguè et al., 2019), Austria (Duethmann and Blöschl, 2018), Southeast Australia (Helfer et al., 2012; Fuentes et al., 2020), in the Brazilian Cerrado (Althoff et al., 2019), Czech Republic (Mozny et al., 2020) and in other parts of the world, generally associated with countries or regions with low rates of gas-emissions/industrialization (Wang et al., 2014; Miralles et al., 2014). These different trends of increase and decrease in evaporation in various regions of the planet have been called an "evaporation paradox" (Brutsaert and Parlange, 1998).

Fu et al. (2009) concluded that three main causes may be directly affecting evaporation, solar radiation, relative humidity and wind speed, that have changed over the last 50 years. The magnitude of the changes and the importance of each of these three variables vary from region to region, creating a different evaporation trend for each area. This trend of evaporation, positive or negative, will also depend on the climatological factor that has the greatest influence/correlation (R^2) on local evaporation and how it has changed over the years.

As previously noted, the evaporation of the reservoirs does not depend only on changes in air temperature, other variables influence this process, such as humidity, wind speed and net radiation (Friedrich et al., 2018). Although global trends in humidity are almost imperceptible, some variations can be better observed on a regional scale. A downward trend (−1.25% per decade, 1976 to 2004) is evident in the Southern Hemisphere (Northeast Brazil) (Dai, 2006). Trends in wind speed on a global scale were also observed (McVicar et al., 2012). In particular, the term "global stilling" is often used to describe the phenomenon of declining global wind speed: an average reduction trend in South America was −0.50 m/s, from 1950 to 2000 (McVicar et al., 2012). Thus, these trends in climatological data should lead to a decrease in evaporation (McVicar et al., 2012; Vautard et al., 2010).

Changes in the climatological variables of the study area were also observed during the 34 years of the present analysis (Table 2). The increase of 0.57 °C in air temperature over 34 years is similar to that found by Hansen et al. (2010) (+0.50 °C) and by the Intergovernmental Panel on Climate Change - IPCC (2013) (+0.70 °C) from 1951 to 2012. Wind speed demonstrated a negative trend of −0.29 m/s in 34 years, slightly below that reported by McVicar et al. (2012) (−0.50 m/s). The relative humidity also exhibited a negative trend of −4.83% in 34 years, close to that reported by Dai (2006) (−5.00%) (Fig. 9).

As noted, the variables wind speed and relative humidity presented the highest correlations with evaporation (R^2 = 0.31–0.42). As expected, evaporation increased with wind speed (positive correlation), but reduced with humidity (negative correlation). In addition to the aforementioned phenomenon of "global dimming", the reduction in

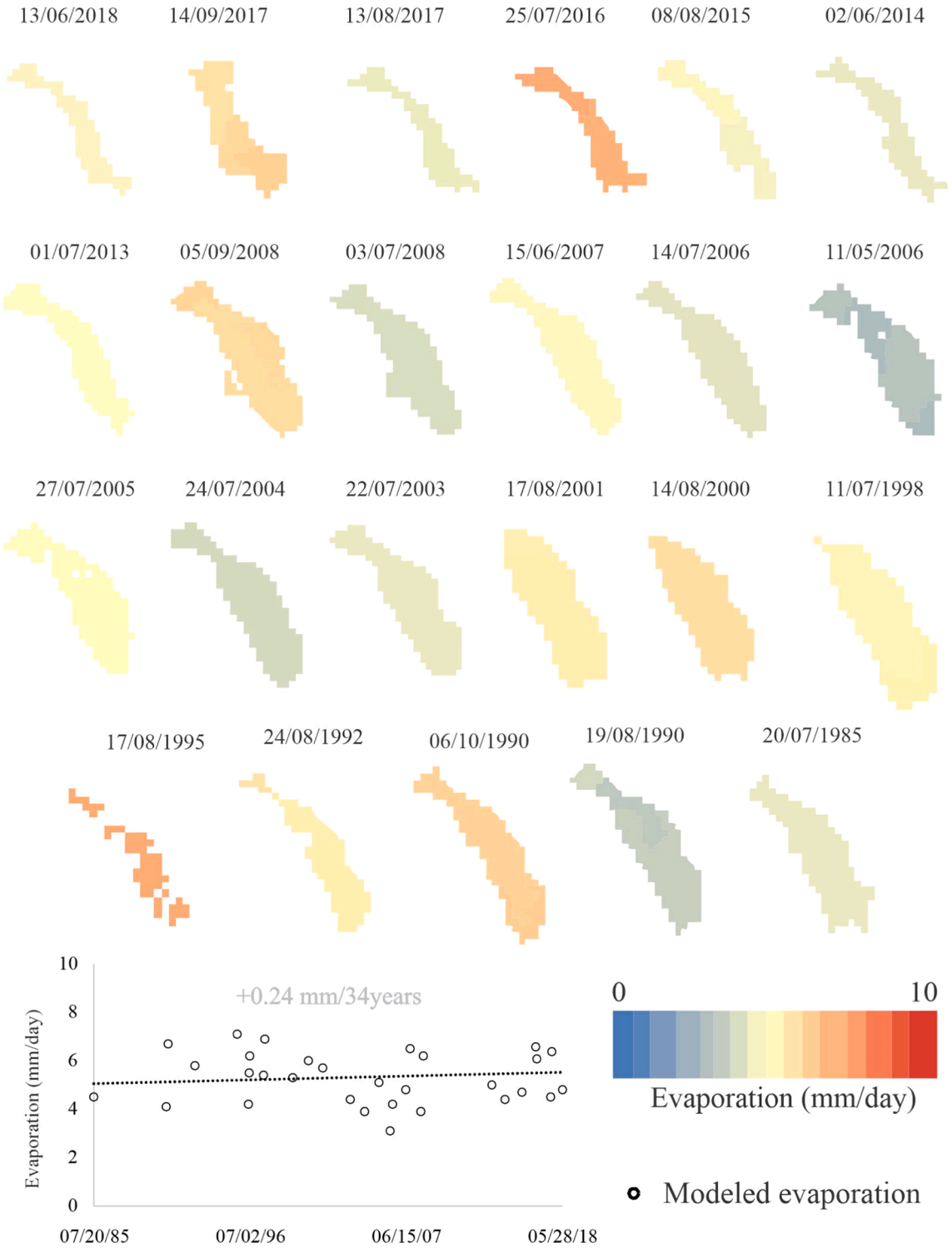

Fig. 5. Trends of evaporation of the Santo Anastácio reservoir (1985 – 2018).

evaporation over Gavião, Riachão and Pacoti reservoirs may be due to a counterbalancing effect of wind speed over humidity on the trend of local evaporation.

3.3. Uncertainty analysis

Although the AquaSEBS model simulations compared favorably with reference data, several sources of uncertainty may be present: i) remote sensing data - emissivity, surface albedo, temperature of the water surface and latent heat flux (λE_{wet}), ii) radiation variables - incoming shortwave and long-wave radiation, iii) meteorological data - air temperature, relative humidity and wind speed, iv) satellite sensor limitations, and v) limited number of scenes (see Timmermans et al. 2013).

Regarding the emissivity and albedo inputs, the uncertainties are thought to small due to their low daily fluctuation, ranging from 1.30 to 2.50% (Ferguson et al. 2010). Furthermore, the AquaSEBS model is not highly sensitive to changes in these variables (Abdelrady et al. 2016).

The surface temperature of the water is estimated from the Landsat

Fig. 6. Trends of evaporation of the Gavião reservoir (1985 – 2018).

TM and OLI sensor images. Uncertainties in this variable are mainly due to the diurnal variability of surface temperature, which can generate large changes in the evaporation estimated by the AquaSEBS because this is one of the most sensitive model variables (Abdelrady et al. 2016). The deeper the lake, the less susceptible it is to large temperature changes, as these have greater energy storage capacity when compared to shallower lakes (Campos et al. 2016a). Therefore, there is greater confidence in surface temperatures for large reservoirs relative to small reservoirs.

There is also uncertainty in estimating the latent heat flux (λE_{wet}), net radiation flux (R_n), water heat flux (G_0) and sensible heat flux (H_{wet}). In estimating R_n there are errors in the short and long wave components (Bisht et al., 2005; Kalma et al., 2008). According to Abdelrady et al. (2016) the main uncertainties of the AquaSEBS model are related to G_0,

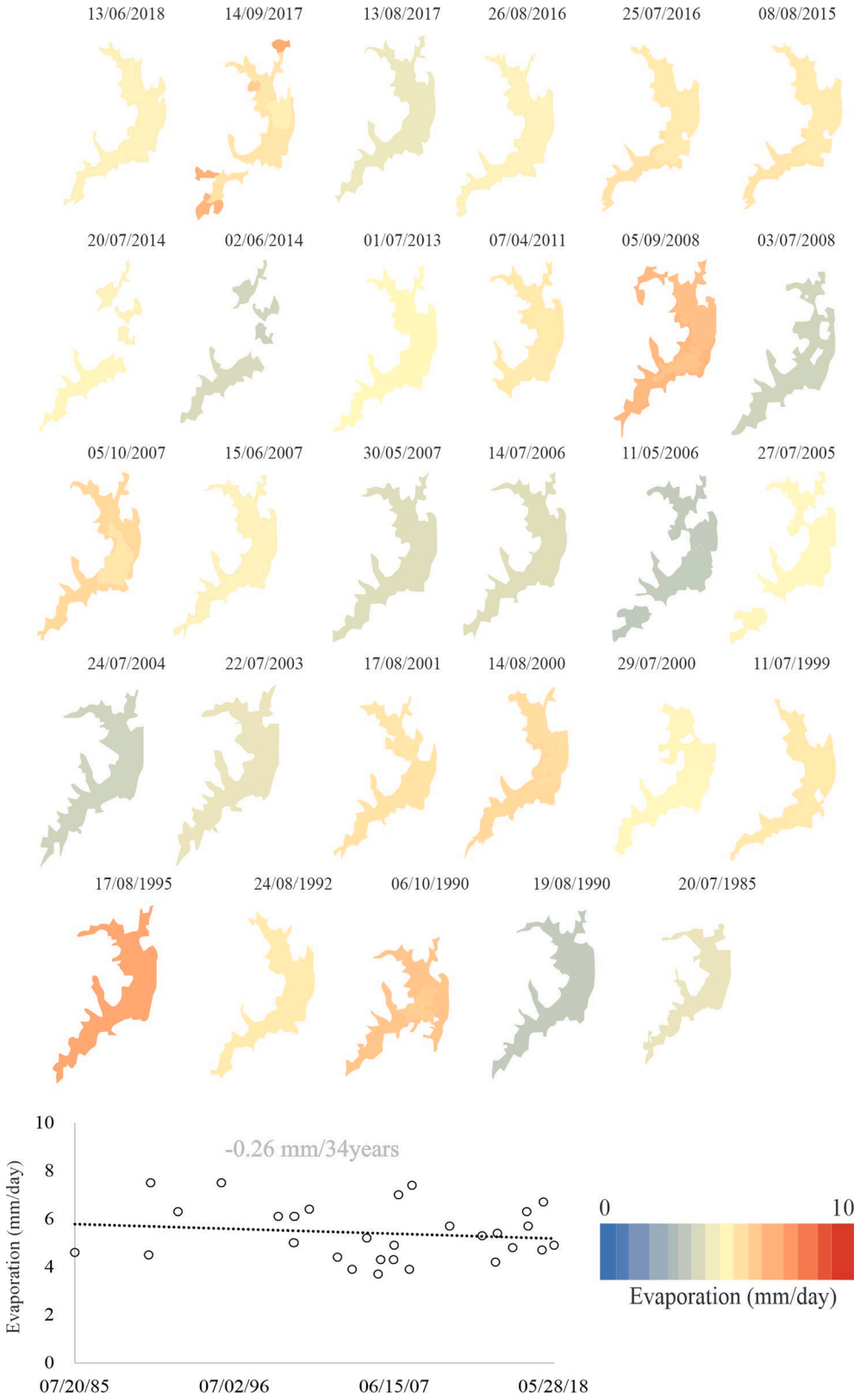

Fig. 7. Trends of evaporation of the Riachão reservoir (1985 – 2018).

whereas there are no major errors in estimating the H_{wet}. Errors in estimating the λE_{wet} can vary between 10 and 30% (Wilson et al., 2002). Regarding λE_{wet}, it is possible to estimate the instantaneous evaporation flux (evaporation value at the time of the satellite's passage), which is considered by AquaSEBS as constant throughout the day, then extrapolating this value to a daily evaporation rate (Abdelrady et al., 2016).

The uncertainty in G_0 is justified by the number of meteorological variables required to estimate it (Abdelrady et al., 2016). The time and location of the measurements of air temperature, wind speed and

Fig. 8. Trends of evaporation of the Pacoti reservoir (1985 – 2018).

relative humidity, as well as the spatial representativeness of these data, are critical (Kalma et al., 2008).

Another source of uncertainty might come from the satellite imagery. Some sensors provide good spatial resolution of the thermal band but at a lower temporal resolution (Landsat 8 - Resolution: spatial thermal band = 100 m; temporal = 16 days; radiometric = 16 bits; spectral = 0.430–12.510 nm). Another important issue for remote sensing is the presence of clouds, often making it impossible to capture the scene in the study area.

An approach to mitigate intermittent cloud cover is to use data from different satellite sensors, although there might be significant differences in their technical characteristics. Coelho et al. (2017) used

Table 2
Trend analysis of climatological variables, modeled (AquaSEBS) and reference (class A pan Kp 0.7 and Penman-Monteith) evaporation.

	Variable	Temperature (°C)	Humidity (%)	Wind speed (m/s)	AquaSEBS Evaporation (mm/34 years)				Class A pan	Penman-Monteith
					Santo Anastácio	Gavião	Riachão	Pacoti	(mm/34 years)	
	Min.	18.5	43.0	0.1	2.4	2.0	2.5	2.1	0.2	5.3
	Mean	27.9	72.9	3.7	5.1	5.0	5.0	5.1	5.1	6.5
	Max.	38.9	100.0	8.5	6.9	7.8	7.8	8.9	12.5	8.4
	τ	0.125	−0.122	−0.054	0.026	−0.027	−0.040	−0.016	0.053	0.014
	S	9,575,969	−9355047	−4001944	7.000	−10.000	−15.000	−6.000	2,438,519	8.000
	p-value	<0.0001*	<0.0001*	<0.0001*	0.882	0.859	0.782	0.921	<0.0001*	0.921
	Slope	0.573	−4.831	−0.292	0.240	−0.140	−0.260	−0.080	0.433	0.303
Time trend	100	1.684	−14.211	−0.860	0.702	−0.417	−0.774	−0.247	1.273	0.892
	500	8.421	−71.054	−4.297	3.510	−2.083	−3.869	−1.234	6.363	4.462

Max. – Maximum; Min. – Minimum; * - There is a significant positive temporal trend at the 5% level; S and τ - indicate the trend (negative or positive); Slope - represents the 34 years increase/decrease of the variable; p-value - is the trend significance < 0.05 high significance.

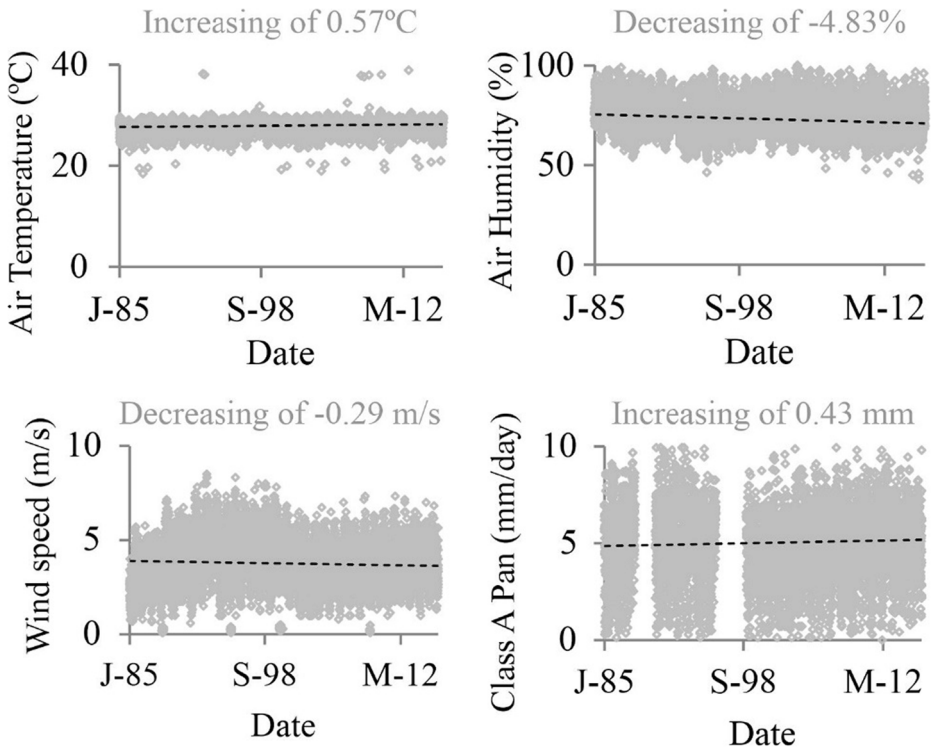

Fig. 9. Variation of air temperature (a), wind speed (b), humidity (c) and class A pan evaporation (Kp 0.7) (d) (1985 – 2018).

multispectral data from Landsat 8 and RapidyEye satellites to analyze water quality in three small reservoirs in the Brazilian semiarid region. Vinukollu et al. (2011) estimated evapotranspiration in various regions of the planet using data from AIRS, AVHRR, CERES, MODIS and NOAA satellites.

AquaSEBS was developed from SEBS (Su et al. 2002), which was intended for evapotranspiration estimation over vegetation and not water. SEBS also has a known tendency to underestimate evaporation in high-temperature areas (Rwasoka et al., 2011; Gokool et al., 2017) such as tropical-coastal Northeast Brazil. This deficiency in the original model (SEBS) may influence the modelled evaporation from AquaSEBS in this type of environment.

Finally, the number of scenes can be a source of error. For instance, the Santo Anastácio reservoir obtained a reasonable temporal characterization compared to measured data, even with fewer scenes than the Gavião, Riachão and Pacoti reservoirs. Therefore, if 23 scenes (Santo Anastácio) resulted in a good trend, it is expected that with 29 (other reservoirs), the analysis would present reasonable trends too.

4. Conclusion

In this study we analyzed temporal trends of evaporation in four reservoirs located in the Brazilian Northeast through remote sensing (RS) by using AquaSEBS model for a 34 year-period. The results indicated that the model performed well, with acceptable levels of error and uncertainty (RMSE $\leq$ 1.25 mm/day, PBIAS $\leq$ 13.7% and $R^2 \geq 0.51$). One reservoir presented a positive trend of evaporation (+0.24 mm/34 years), corroborating the measurements of a reference Class A pan and Penman-Monteith estimates, while the others presented negative trends (−0.26 to −0.080 mm/34 years). The different behavior was attributed to the impact of regional air pollution, analogous to the global dimming effect of reducing evaporation in reservoirs located closer to industrial areas. The trends in air temperature, relative humidity and wind speed were also analyzed. Temperature presented a positive trend over time (+0.57 °C/34 years), while humidity (−4.83%) and wind speed (−0.29 m/s) presented negative trends. Moderate correlations ($R^2 > 0.31$) were also obtained between evaporation rates and wind speed or humidity. A decreasing evaporation trend will result in reduced water losses from reservoir volumes, and is thus an important result from a water resource

planning perspective.

Further research is needed to increase the precision and confidence in AquaSEBS model outputs. A sensitivity analysis could be implemented to assess which variables and parameters have the greatest influence on model output, and to enhance the calibration routine. Finally, the results obtained here contributed to a better understanding of the evaporation rates and trends in Brazilian tropical reservoirs and their relationships with relevant climatological variables, and can support water resources planning and management in this water-scarce region.

Declaration of Competing Interest

The authors declare that they have no known competing financial interests or personal relationships that could have appeared to influence the work reported in this paper.

Acknowledgment

The authors would like to thank Coordination for the Improvement of Higher Education Personnel (CAPES/CNPq) for the resources granted to the second and third authors. We also thank FUNCAP (Cearense Foundation for Support for Scientific and Technological Development) for the scholarship granted to the first author.

References

Abdelrady, A., Timmermans, J., Vekerdy, Z., Salama, M., 2016. Surface energy balance of fresh and saline waters: AquaSEBS. Remote Sens. 8 (7), 583.

Allen, R., Tasumi, M., Trezza, R., Waters, R., and Bastiaanssen, W. (2002). SEBAL (Surface Energy Balance Algorithms for Land)—Advanced Training and Users Manual - Idaho Implementation (Version 1.0). The Idaho Department of Water Resources: Boise, ID, USA.

Al-Shammiri, M., 2002. Evaporation rate as a function of water salinity. Desalination 150 (2), 189–203.

Althoff, D., Rodrigues, L.N., da Silva, D.D., 2019. Evaluating evaporation methods for estimating small reservoir water surface evaporation in the brazilian savannah. Water 11 (9), 1942.

Andrade, E.M., Guerreiro, M.J.S., Palácio, H.A.Q., Campos, D.A., 2020. Ecohydrology in a Brazilian tropical dry forest: thinned vegetation impact on hydrological functions and ecosystem services. J. Hydrol.: Reg. Stud. 27, 100649.

Araújo, G.M., Lima Neto, I.E., 2018. Removal of Organic Matter in Stormwater Ponds: A Plug-flow Model Generalisation from Waste Stabilisation Ponds to Shallow Rivers. Urban Water J. 15 (9), 918–924. https://doi.org/10.1080/1573062X.2019.1581231.

Araújo, G.M., Lima Neto, I.E., Becker, H. (2019). Phosphorus Dynamics in a Highly Polluted Urban Drainage Channel Shallow Reservoir System in the Brazilian Semiarid. Annals of the Brazilian Academy of Sciences 91 (3). doi:10.1590/0001-3765201920180441.

Avdan, U., Jovanovska, G. (2016). Algorithm for automated mapping of land surface temperature using LANDSAT 8 satellite data. Journal of Sensors, 2016.

Bastiaanssen, W.G.M., 2000. SEBAL-based sensible and latent heat fluxes in the irrigated Gediz Basin, Turkey. J. Hydrol. 229 (1-2), 87–100.

Bastiaanssen, W.G.M., Menenti, M., Feddes, R.A., Holtslag, A.A.M., 1998. A remote sensing surface energy balance algorithm for land (SEBAL). 1. Formulation. J. Hydrol. 212-213, 198–212.

Bisht, G., Venturini, V., Islam, S., Jiang, L.e., 2005. Estimation of the net radiation using MODIS (Moderate Resolution Imaging Spectroradiometer) data for clear sky days. Remote Sens. Environ. 97 (1), 52–67.

Brutsaert, W., and Parlange, M. B. (1998). Hydrologic cycle explains the evaporation paradox. Nature, 396(6706), 30.

Burn, D.H., Hesch, N.M., 2007. Trends in evaporation for the Canadian Prairies. J. Hydrol. 336 (1-2), 61–73.

Campos, J.N.B., Lima Neto, I.E., Studart, T.M.C., Nascimento, L.S.V., 2016a. Trade-off between reservoir yield and evaporation losses as a function of lake morphology in semi-arid Brazil. Annals of the Brazilian Academy of Sciences 88 (2), 1113–1125.

Campos, W.W., Gaspar, J., de Oliveira Lage, M., Kawashima, R.S., Giannotti, M.A., Quintanilha, J.A., 2016b. Avaliação de classificadores de imagem de satélite a partir do uso de uma técnica de votação. Revista Brasileira de Cartografia 68 (8).

Chandler, G., Markham, B., 2003. Revised Landsat-5 TM radiometric calibration procedures and post calibration dynamic ranges: IEEE Transactions Geoscience Remote Sensing. Piscataway 41 (11).

Chattopadhyay, N., Hulme, M., 1997. Evaporation and potential evapotranspiration in India under conditions of recent and future climate change. Agric. For. Meteorol. 87 (1), 55–73.

Coelho, C., Heim, B., Foerster, S., Brosinsky, A., de Araújo, J., 2017. In situ and satellite observation of CDOM and Chlorophyll-a dynamics in small water surface reservoirs in the Brazilian semiarid region. Water 9 (12), 913.

COGERH – Companhia de Gestão de Recursos Hídricos, FUNCEME – Fundação Cearense de Metrologia e Recursos Hídricos, Portal Hidrológico do Ceará, 2020. http://www.hidro.ce.gov.br/.

Cohen, S., Ianetz, A., Stanhill, G., 2002. Evaporative climate changes at bet Dagan, Israel, 1964–1998. Agric. For. Meteorol. 111 (2), 83–91.

Dai, A., 2006. Recent climatology, variability, and trends in global surface humidity. J. Clim. 19, 3589–3606.

Downing, J.A., Prairie, Y.T., Cole, J.J., Duarte, C.M., Tranvik, L.J., Striegl, R.G., McDowell, W.H., Kortelainen, P., Caraco, N.F., Melack, J.M., Middelburg, J.J., 2006. The global abundance and size distribution of lakes, ponds, and impoundments. Limnol. Oceanogr. 51 (5), 2388–2397.

Duethmann, D., Blöschl, G., 2018. Why has catchment evaporation increased in the past 40 years? A data-based study in Austria. Hydrol. Earth Syst. Sci. 22 (10).

Ferguson, C.R., Sheffield, J., Wood, E.F., Gao, H., 2010. Quantifying uncertainty in a remote sensing-based estimate of evapotranspiration over continental USA. Int. J. Remote Sens. 31 (14), 3821–3865.

Finch, J., Calver, A., 2008. Methods for the quantification of evaporation from lakes (prepared for the World Meteorological Organization's Commission for Hydrology). Oxford shire, UK.

Finch, J.W., Hall, R.L., 2001. Estimation of open water evaporation: A review of methods. Environment Agency, Bristol, UK.

Fraga, R.F., Rocha, S.M.G., Lima Neto, I.E., 2020. Impact of flow conditions on coliform dynamics in an urban lake in the Brazilian semiarid. Urban Water J. 17 (1), 43–53.

Freitas, L. C. L. (2016). A qualidade do ar na região metropolitana de Fortaleza - CE sob a perspectiva do sistema clima urbano. PhD Thesis. Federal University of Ceará - UFC, 197 p (in Portuguese).

Friedrich, K., Grossman, R.L., Huntington, J., Blanken, P.D., Lenters, J., Holman, K.D., Gochis, D., Livneh, B., Prairie, J., Skei, E., Healey, N.C., Dahm, K., Pearson, C., Finnessey, T., Hook, S.J., Kowalski, T., 2018. Reservoir evaporation in the Western United States: current science, challenges, and future needs. Bull. Am. Meteorol. Soc. 99 (1), 167–187.

Fu, G., Charles, S.P., Yu, J., 2009. A critical overview of pan evaporation trends over the last 50 years. Clim. Change 97 (1–2), 193.

Fuentes, I., van Ogtrop, F., Vervoort, R.W., 2020. Long-term surface water trends and relationship with open water evaporation losses in the Namoi catchment. Australia. Journal of Hydrology 584, 124714. https://doi.org/10.1016/j.jhydrol.2020.124714.

Gokool, S., Jarmain, C., Riddell, E., Swemmer, A., Lerm, R., Chetty, K.T., 2017. Quantifying riparian total evaporation along the Groot Letaba River: A comparison between infilled and spatially downscaled satellite derived total evaporation estimates. J. Arid Environ. 147, 114–124.

Guo, Y., Zhang, Y., Ma, N., Xu, J., Zhang, T., 2019. Long-term changes in evaporation over Siling Co Lake on the Tibetan Plateau and its impact on recent rapid lake expansion. Atmos. Res. 216, 141–150.

Gupta, H.V., Sorooshian, S., Yapo, P.O., 1999. Status of automatic calibration for hydrologic models: Comparison with multilevel expert calibration. J. Hydrol. Eng. 4 (2), 135–143.

Hansen, J., Ruedy, R., Sato, M., Lo, K., 2010. Global surface temperature change. Rev. Geophys. 48 (4) https://doi.org/10.1029/2010RG000345.

Harmsen, E.W., González-Pérez, A., Winter, A., 2004. Re-evaluation of pan evaporation coefficients at seven locations in Puerto Rico. The Journal of Agriculture of the University of Puerto Rico 88 (3–4), 109–122.

Havens, K.E., Ji, G., 2018. Multiyear oscillations in depth affect water quality in Lake Apopka. Inland Waters 8 (1), 1–9.

Helfer, F., Lemckert, C., Zhang, H., 2012. Impacts of climate change on temperature and evaporation from a large reservoir in Australia. J. Hydrol. 475, 365–378.

Hounguè, R., Lawin, A.E., Moumouni, S., Afouda, A.A., 2019. Change in Climate Extremes and Pan Evaporation Influencing Factors over Ouémé Delta in Bénin. Climate 7 (1), 2.

Intergovernmental Panel on Climate Change - IPCC, 2013. Climate change 2013: the physical science basis Contribution of Working Group I to the Fifth Assessment Report of the Intergovernmental Panel on Climate Change. Cambridge University Press, New York, p. 1552.

Instituto Nacional de Meteorologia – INMET. Normais Climatológicas do Brasil. 2019. http://www.inmet.gov.br/projetos/rede/pesquisa/inicio.php. Acessado em 16 de Dezembro de 2019.

IPECE - Instituto de Pesquisa e Estratégia Econômica do Ceará – Indústria de transformação ativa - 2017. Disponible: http://www2.ipece.ce.gov.br/atlas/capitulo5/52/pdf/Industria_transformacao_Ativa_2017.pdf Accessed 14 February 2020.

IPECE - Instituto de Pesquisa e Estratégia Econômica do Ceará. Perfil Básico Municipal. 2018. <http://www.ipece.ce.gov.br/index.php/perfil-municipal-2018>. Accessed: 03 July 2019.

Jin, Z., Charlock, T.P., Smith, W.L., Rutledge, K., 2004. A parameterization of ocean surface albedo. Geophys. Res. Lett. 31 (22) https://doi.org/10.1029/2004GL021180.

Kalma, J.D., McVicar, T.R., McCabe, M.F., 2008. Estimating land surface evaporation: A review of methods using remotely sensed surface temperature data. Surv. Geophys. 29 (4-5), 421–469.

Kendall, M.G., 1975. Rank Correlation Measures. Charles Griffin, London.

Konapala, G., Mishra, A.K., Wada, Y., Mann, M.E., 2020. Climate change will affect global water availability through compounding changes in seasonal precipitation and evaporation. Nat. Commun. 11 (1), 1–10.

Lawrimore, J.H., Peterson, T.C., 2000. Pan evaporation trends in dry and humid regions of the United States. J. Hydrometeorol. 1 (6), 543–546.

Lima Neto, I.E., 2019. Impact of artificial destratification on water availability of reservoirs in the Brazilian semiarid. Ann. Braz. Acad. Sci. 91 (3), 1–12.

Lima Neto, I.E., Wiegand, M.C., de Araújo, J.C., 2011. Sediment redistribution due to a dense reservoir network in a large semi-arid Brazilian basin. Hydrol. Sci. J. 56 (2), 319–333.
Linacre, E.T., 1994. Estimating US Class A pan evaporation from few climate data. Water Int. 19 (1), 5–14.
Liu, B., Xu, M., Henderson, M., Gong, W., 2004. A spatial analysis of pan evaporation trends in China, 1955–2000. Journal of Geophysical Research: Atmospheres 109 (D15).
Zamani Losgedaragh, S., Rahimzadegan, M., 2018. Evaluation of SEBS, SEBAL, and METRIC models in estimation of the evaporation from the freshwater lakes (Case study: Amirkabir dam, Iran). J. Hydrol. 561, 523–531.
Maclean, I.M.D., Suggitt, A.J., Wilson, R.J., Duffy, J.P., Bennie, J.J., 2017. Fine-scale climate change: modelling spatial variation in biologically meaningful rates of warming. Glob. Change Biol. 23 (1), 256–268.
Malaret, E., Bartolucci, L.A., Lozano, D.F., Anuta, P.E., Mcgillem, C.D., 1985. Landsat-4 and Landsat-5 Thematic Mapper data quality analysis. Photogramm. Eng. Remote Sens. 51 (9), 1407–1416.
Mamede, G.L., Guentner, A., Medeiros, P.H.A., de Araújo, J.C., Bronstert, A., 2018. Modeling the effect of multiple reservoirs on water and sediment dynamics in a semiarid catchment in Brazil. J. Hydrol. Eng. 23 (12), 05018020. https://doi.org/10.1061/(ASCE)HE.1943-5584.0001701.
Mann, H.B., 1945. Nonparametric tests against trend. Econometrica 13 (3), 245. https://doi.org/10.2307/1907187.
McJannet, D.L., Cook, F.J., Burn, S., 2013. Comparison of techniques for estimating evaporation from an irrigation water storage. Water Resour. Res. 49 (3), 1415–1428.
McMahon, T.A., Finlayson, B.L., Peel, M.C., 2016. Historical developments of models for estimating evaporation using standard meteorological data. Wiley Interdisciplinary Reviews: Water 3 (6), 788–818.
McVicar, T.R., Roderick, M.L., Donohue, R.J., Li, L.T., Van Niel, T.G., Thomas, A., Grieser, J., Jhajharia, D., Himri, Y., Mahowald, N.M., Mescherskaya, A.V., Kruger, A. C., Rehman, S., Dinpashoh, Y., 2012. Global review and synthesis of trends in observed terrestrial near-surface wind speeds: Implications for evaporation. J. Hydrol. 416-417, 182–205.
Mesquita, J.B.d.F., Lima Neto, I.E., Raabe, A., de Araújo, J.C., 2020. The influence of hydroclimatic conditions and water quality on evaporation rates of a tropical lake. J. Hydrol. 590, 125456. https://doi.org/10.1016/j.jhydrol.2020.125456.
Metzger, J., Nied, M., Corsmeier, U., Kleffmann, J., Kottmeier, C., 2018. Dead Sea evaporation by eddy covariance measurements vs. aerodynamic, energy budget, Priestley-Taylor, and Penman estimates. Hydrol. Earth Syst. Sci. 22 (2), 1135–1155.
Miralles, D.G., van den Berg, M.J., Gash, J.H., Parinussa, R.M., de Jeu, R.A.M., Beck, H. E., Holmes, T.R.H., Jiménez, C., Verhoest, N.E.C., Dorigo, W.A., Teuling, A.J., Johannes Dolman, A., 2014. El Niño–La Niña cycle and recent trends in continental evaporation. Nat. Clim. Change 4 (2), 122–126.
Missions, U. L. (2016). Using the USGS Landsat8 Product. US Department of the Interior-US Geological Survey–NASA.
Moonen, A. C., Ercoli, L., Mariotti, M., andMasoni, A. (2002). Climate change in Italy indicated by agrometeorological indices over 122 years. Agricultural and Forest Meteorology, 111(1), 13-27.
Rong, Y., Su, H., Zhang, R., and Duan, Z. (2013). Effects of climate variability on evaporation in Dongping Lake, China, during 2003–2010. Advances in Meteorology, 2013.
Moriasi, D. N., Arnold, J. G., Van Liew, M. W., Bingner, R. L., Harmel, R. D., andVeith, T. L. (2007). Model evaluation guidelines for systematic quantification of accuracy in watershed simulations. Transactions of the ASABE, 50(3), 885-900.
Morton, F.I., 1986. Practical estimates of lake evaporation. J. Climate Appl. Meteorol. 25 (3), 371–387.
Mozny, M., Trnka, M., Vlach, V., Vizina, A., Potopova, V., Zahradnicek, P., Stepanek, P., Hajkova, L., Staponites, L., Zalud, Z., 2020. Past (1971–2018) and future (2021–2100) pan evaporation rates in the Czech Republic. J. Hydrol. 590, 125390. https://doi.org/10.1016/j.jhydrol.2020.125390.
Nouri, M., Homaee, M., Bannayan, M., 2017. Quantitative trend, sensitivity and contribution analyses of reference evapotranspiration in some arid environments under climate change. Water Resour. Manage. 31 (7), 2207–2224.
Ohmura, A., Wild, M., 2002. Is the hydrological cycle accelerating? Science 298 (5597), 1345–1346.
Ozdogan, M., Salvucci, G.D., 2004. Irrigation-induced changes in potential evapotranspiration in southeastern Turkey: Test and application of Bouchet's complementary hypothesis. Water Resour. Res. 40 (4) https://doi.org/10.1029/2003WR002822.
Penman, H.L., 1948. Natural evaporation from Open Water, bare soil and grass. Proc, Roy, SOC, London, A 193, 120–145.
Peterson, T.C., Golubev, V.S., Groisman, P.Y., 1995. Evaporation losing its strength. Nature 377 (6551), 687–688.
Pourmansouri, F., Rahimzadegan, M., 2020. Evaluation of vegetation and evapotranspiration changes in Iran using satellite data and ground measurements. J. Appl. Remote Sens. 14 (3), 034530.
Roderick, M.L., Farquhar, G.D., 2004. Changes in Australian pan evaporation from 1970 to 2002. International Journal of Climatology: A Journal of the Royal Meteorological Society 24 (9), 1077–1090.
Roderick, M.L., Farquhar, G.D., 2005. Changes in New Zealand pan evaporation since the 1970s. International Journal of Climatology: A Journal of the Royal Meteorological Society 25 (15), 2031–2039.
Rwasoka, D.T., Gumindoga, W., Gwenzi, J., 2011. Estimation of actual evapotranspiration using the Surface Energy Balance System (SEBS) algorithm in the Upper Manyame catchment in Zimbabwe. Physics and Chemistry of the Earth, Parts A/B/C 36 (14-15), 736–746.
Silva, B.B.da., Braga, A.C., Braga, Célia.C., Oliveira, L.M.M.de., Montenegro, S.M.G.L., Barbosa Junior, B., 2016. Procedures for calculation of the albedo with OLI-Landsat 8 images: Application to the Brazilian semi-arid. Revista Brasileira de Engenharia Agrícola e Ambiental 20 (1), 3–8.
Senay, G.B., Schauer, M., Friedrichs, M., Velpuri, N.M., Singh, R.K., 2017. Satellite-based water use dynamics using historical Landsat data (1984–2014) in the southwestern United States. Remote Sens. Environ. 202, 98–112.
Shelquist, R., 2009. Equations-air density and density altitude. Equations-Air Density and Density Altitude.
Stanhill, G., Cohen, S., 2001. Global dimming: a review of the evidence for a widespread and significant reduction in global radiation with discussion of its probable causes and possible agricultural consequences. Agric. For. Meteorol. 107 (4), 255–278.
Su, Z., 2002. The Surface Energy Balance System (SEBS) for estimation of turbulent heat fluxes. Hydrol. Earth Syst. Sci. 6 (1), 85–99.
Tasumi, M. Progress in operational estimation of regional evapotranspiration using satellite imagery. 357p., (Dissertation Doctor of Philosophy). University of Idaho, 2003.
Tebakari, T., Yoshitani, J., Suvanpimol, C. (2005). Time-space trend analysis in pan evaporation over Kingdom of Thailand. Journal of Hydrologic Engineering, 10(3), 205-215.
Timmermans, J., Su, Z., van der Tol, C., Verhoef, A., Verhoef, W., 2013. Quantifying the uncertainty in estimates of surface-atmosphere fluxes through joint evaluation of the SEBS and SCOPE models. Hydrol. Earth Syst. Sci. 17 (4), 1561–1573.
Vautard, R., Cattiaux, J., Yiou, P., Thépaut, J.-N., Ciais, P., 2010. Northern Hemisphere atmospheric stilling partly attributed to an increase in surface roughness. Nat. Geosci. 3 (11), 756–761.
Vinukollu, R.K., Wood, E.F., Ferguson, C.R., Fisher, J.B., 2011. Global estimates of evapotranspiration for climate studies using multi-sensor remote sensing data: Evaluation of three process-based approaches. Remote Sens. Environ. 115 (3), 801–823.
Wang, W., Xiao, W., Cao, C., Gao, Z., Hu, Z., Liu, S., Shen, S., Wang, L., Xiao, Q., Xu, J., Yang, D., Lee, X., 2014. Temporal and spatial variations in radiation and energy balance across a large freshwater lake in China. J. Hydrol. 511, 811–824.
Wilson, K., Goldstein, A., Falge, E., Aubinet, M., Baldocchi, D., Berbigier, P., Bernhofer, C., Ceulemans, R., Dolman, H., Field, C., Grelle, A., Ibrom, A., Law, B.E., Kowalski, A., Meyers, T., Moncrieff, J., Monson, R., Oechel, W., Tenhunen, J., Valentini, R., Verma, S., 2002. Energy Balance Closure at FLUXNET Sites. Agric. For. Meteorol. 113 (1-4), 223–243.
Xu, J., Haginoya, S., Saito, K., Motoya, K., 2005. Surface heat balance and pan evaporation trends in Eastern Asia in the period 1971–2000. Hydrological Processes: An Int. J. 19 (11), 2161–2186.
Xu, S., Yu, Z., Yang, C., Ji, X., Zhang, K., 2018. Trends in evapotranspiration and their responses to climate change and vegetation greening over the upper reaches of the Yellow River Basin. Agric. For. Meteorol. 263, 118–129.
Zhao, G., Gao, H., 2019. Estimating reservoir evaporation losses for the United States: Fusing remote sensing and modeling approaches. Remote Sens. Environ. 226, 109–124.